Small suppression of the complete fusion of the ^{6}Li + ^{96}Zr system at near-barrier energies

S. P. Hu,[1,3] G. L. Zhang,[2,*] J. C. Yang,[2] H. Q. Zhang,[1,†] P. R. S. Gomes,[4] J. Lubian,[4] X. G. Wu,[1] J. Zhong,[1,3] C. Y. He,[1] Y. Zheng,[1] C. B. Li,[1] G. S. Li,[1] W. W. Qu,[2] F. Wang,[2] L. Zheng,[2] L. Yu,[2] Q. M. Chen,[1] P. W. Luo,[1,3] H. W. Li,[1,5] Y. H. Wu,[1,5] W. K. Zhou,[1] B. J. Zhu,[1] and H. B. Sun[3]

[1]*China Institute of Atomic Energy, Beijing 102413, China*

[2]*School of Physics and Nuclear Energy Engineering, Beihang University, Beijing 100191, China*

[3]*College of Physics Science and Technology, Shenzhen University, Shenzhen 518060, China*

[4]*Instituto de Física, Universidade Federal Fluminense, Avenida Litoranea s/n, Gragoatá, Niterói, Rio de Janeiro 24210-340, Brazil*

[5]*College of Physics, Jilin University, Changchun 130012, China*

(Received 24 December 2014; revised manuscript received 12 March 2015; published 30 April 2015)

The measurements of complete fusion cross sections for ^{6}Li + ^{96}Zr have been performed at energies around the Coulomb barrier by the online γ-ray method. The complete fusion cross sections at above-barrier energies were found to be suppressed by ∼25%. A comparison of the systematics of complete fusion suppression with the existing data for ^{6}Li+ heavy targets with the present results shows that the systematics of the suppression factor observed for ^{6}Li-induced fusion in the heavy mass region may not be consistent in lighter target mass region.

DOI: 10.1103/PhysRevC.91.044619 PACS number(s): 25.60.Pj, 25.60.Gc, 25.70.Gh, 25.70.Jj

I. INTRODUCTION

The investigation of the breakup effect of weakly bound nuclei on the fusion process has been an interesting research topic in the past several years [1,2]. Several experiments and theoretical calculations have focused on this subject. For tightly bound nuclei, the enhancement of fusion cross sections at sub-barrier energies has been successfully explained by one-dimensional barrier penetration models (1DBPM) coupling with inelastic excitations and transfer channels. However, the situation is more complicated when weakly bound nuclei are involved. Different processes can occur after the breakup of weakly bound nuclei (usually the projectiles). When all the fragments fuse with target nucleus, this process is called sequential complete fusion (SCF). When only part of the fragments fuses with the target nucleus, this process is called incomplete fusion (ICF). During the fusion process, the whole projectile can also fuse with the target nucleus without breakup, and this process is named direct complete fusion (DCF). Experimentally, the residues formed in SCF cannot be distinguished from ones from DCF, since the compound nucleus is the same. Therefore, in the experiment the complete fusion (CF) cross sections include the contributions of both SCF and DCF. The total fusion (TF) cross section is equal to the sum of CF and ICF, $\sigma_T = \sigma_{\rm CF} + \sigma_{\rm ICF}$.

Weakly bound nuclei include unstable and stable nuclei. Recently, with the availability of radioactive ion beam (RIB) facilities in a few laboratories, one can produce several kinds of unstable nuclei including neutron- and proton-rich nuclei. Experimental fusion cross sections of unstable nuclei with different target nuclei have been reported. However, owing to the low intensities of the presently available RIB, it is difficult to clearly explore the reaction mechanisms of nuclear systems with unstable nuclei. In comparison with RIB, the beam intensities of stable weakly bound nuclei such as ^{6,7}Li and ^{9}Be, which have significant breakup probability, are orders of magnitude higher. Precise fusion measurements have already been performed with those stable weakly bound nuclei, and the effect of breakup of those nuclei in the fusion process has been extensively studied. Such studies give an important step forward for understanding the influence of breakup in the fusion process. The reported results show that CF cross sections are suppressed at energies slightly above the Coulomb barrier in comparison with 1DBPM coupled-channel calculations, which do not take into account breakup channels. So, the usual conclusion is that this phenomenon of CF suppression arises from the influence of the breakup. Actually, it has been shown [3–5] that the breakup process produces repulsive polarization potential that increases the fusion barrier height and consequently suppresses CF cross section at near-barrier energies. On the other hand, the TF cross sections are not affected by the breakup at the same energy region [6–8], what means that part of the flux that would otherwise produce CF actually produces ICF of the weakly bound projectile. The systematic behavior of the CF cross section suppression of stable weakly bound nuclei, at energies slightly above the Coulomb barrier, has been investigated in some recent papers [9–14]. It was found that the CF suppression factors for reactions induced by the same projectile are independent of the charge of target nuclei and mainly depend only on the breakup threshold energy values of the projectile. The suppression factors found in each paper differ a little from each other, owing to the different bare potentials used in the calculations. Wang *et al.* [14], for ^{6}Li with a breakup threshold energy of 1.474 MeV, found an average suppression around 40%. For ^{7}Li, with threshold of 2.467 MeV, the suppression is around 33%, and for ^{9}Be, with threshold of 1.573 MeV, the suppression is 32%. These results are somehow unexpected, since it is widely accepted that the Coulomb contribution to the total breakup should increase with the charge of the target (Z_t). Indeed, recently Otomar *et al.* [15] showed that the nuclear

*zgl@buaa.edu.cn
†huan@ciae.ac.cn

component of the breakup of ^{6}Li increases linearly with $A_t^{1/3}$ (A_t is the mass of the target) for the same $E_{\mathrm{c.m.}}/V_B$ energy, whereas the Coulomb component increases linearly with Z_t. The total breakup, including the interference between its two components, also increases with the target mass and charge [15]. These behaviors were explained by Hussein *et al.* [16]. A recent possible explanation for this apparent inconsistency of results was given in Refs. [14,17,18]. They claim that the breakup may be of two kinds: prompt and delayed, the first taking place when the projectile is approaching the target and the latter when it is already leaving the target region. As pointed out by Luong *et al.* [19], only the prompt breakup may affect the fusion process. Since in the calculations to derive breakup cross sections, such as the ones performed by Otomar *et al.* [15], they do not separate prompt and delayed breakups, this might explain the apparent contradiction of results. This explanation is based on recent very precise experimental results performed at The Australian National University, where they were able to distinguish prompt and delayed breakups by the determination of their time scales [19,20]. It was found that at sub-barrier energies the breakup following transfer of nucleons (delayed breakup) is dominant over the prompt breakup of ^{6,7}Li. Also, Santra *et al.* [21] and Shrivastava *et al.* [22] performed experiments where it is found that the delayed breakup of ^{6}Li, feeding the long lived resonance 3^{+} at 2.186 MeV of ^{6}Li, predominates in relation to the direct prompt breakup.

Another possible explanation for the apparent independence of the CF suppression with the target mass, and not excluding the previous one, is that so far it was not possible to investigate the effect of breakup on the CF of medium and light targets, when the Coulomb breakup should be much smaller than for heavy targets. The reason for that is the lack of CF measurements of those systems, owing to the characteristics of the evaporation of the relatively light compound nuclei. While the evaporation of heavy systems occurs mainly by the emission of neutrons, for light systems there is a large probability of evaporation of charged particles, and consequently some of the residual nuclei of the CF and ICF coincide. This is the reason why one finds in literature only the measurement of TF of light weakly bound systems. In the present work we aim to explore this second possible explanation. The lightest target for which it was possible to measure CF induced by lithium isotopes is ^{90}Zr [9]. The CF suppression found for this system is 34% or 40% if one follows the study of Wang *et al.* [14]. For CF induced by ^{9}Be, the lightest target is ^{89}Y [23], and the CF suppression was found to be 32%. For lighter targets, only TF cross sections were reported. For ^{6,7}Li projectiles, TF were measured on the targets ^{12}C, ^{27}Al, ^{28}Si, ^{59}Co, and ^{64}Ni [24–32]. For most of the tens of systems for which TF of stable weakly bound nuclei were measured, from light to heavy targets, the results of experiments and coupled channel calculations which do not include the breakup channel coincide [7,8,33]. Only for a few systems it is observed some suppression of TF [24,27,29,30,32]. However, some of these systems were measured by other groups and do not show any suppression [25,26,31]. In a recent and very interesting paper [28], an estimate of CF was obtained for the ^{6}Li + ^{64}Ni by measuring TF and using predictions from evaporation code PACE [34]. The derived CF suppression was $13 \pm 7\%$, much smaller than the 40% suppression found for heavier targets. It is interesting to mention that Kumawat *et al.* [9], who plotted the CF of ^{6}Li with several heavy targets, included the targets ^{28}Si and ^{59}Co, although only TF was obtained for those targets. To answer the question concerning how the breakup affects the CF cross section, one needs more experimental data on medium mass targets.

In this paper we present the measurement of fusion excitation function for the ^{6}Li projectile on a ^{96}Zr target by the online characteristic γ spectrometry method. The present work can estimate the CF cross section by summing the cross sections of dominant neutron evaporation channels and obtain the TF cross sections by adding the contribution of ICF. The derived CF data may contribute to answer the question of suppression of CF cross section on medium mass and light mass targets at energies above the Coulomb barrier. This paper is organized as follows. In Sec. II the experimental details are introduced and the analysis of experimental results are given. In Sec. III the method of derivation of CF and ICF (and TF) is presented and the results are shown. In Sec. IV the coupling channel calculations and the discussion of the breakup effect on fusion are shown. The conclusion is given in Sec. V.

II. EXPERIMENTAL DETAILS

The experiment was carried out with a $^{6}Li^{3+}$ beam at the HI-13 Tandem Accelerator of the China Institute of Atomic Energy (CIAE) in Beijing at bombarding energies from 16 to 28 MeV in steps of 2 MeV. The nominal Coulomb barrier is 17.38 MeV at the laboratory frame (16.36 MeV in the c.m. frame). A 99% enriched $^{96}ZrO_2$ metallic foil with 550 μg/cm^2 thickness and a 1.92 mg/cm^2 gold backing was used. The fusion excitation function was measured using the online characteristic γ spectrometry method. The irradiation times lasted 1–2 h at all energies for the single γ-ray measurements. The beam current was varied from 5.7 to 14.0 enA, and the beam flux was recorded by a Faraday cup mounted behind the target using a precise current integrator device. Two Si(Au) surface barrier detectors were positioned at 30° with respect to the beam direction for verification of the beam intensity and normalization and centrality of the beam. An array consisting of 9 Compton-suppressed BGO-HPGe spectrometers and two planar HpGe detectors was used to detect online γ rays emitted by the reaction products. The absolute efficiency and energy calibration of the detectors were achieved using a set of standard radioactive sources of ^{152}Eu and ^{133}Ba at the target position. The Versa Module Europa (VME)–based data acquisition system MIDAS was used to record the data. The total uncertainty in this experiment mainly came from the statistical errors associated with the yields of the γ rays and from the systematic errors in the target thickness (1%) as well as the estimation of the beam intensity. The typical characteristic γ spectrum for the ^{6}Li+ ^{96}Zr fusion system at $E_{\mathrm{lab}} = 28$ MeV is given in Fig. 1, where several identified channels via complete fusion are denoted.

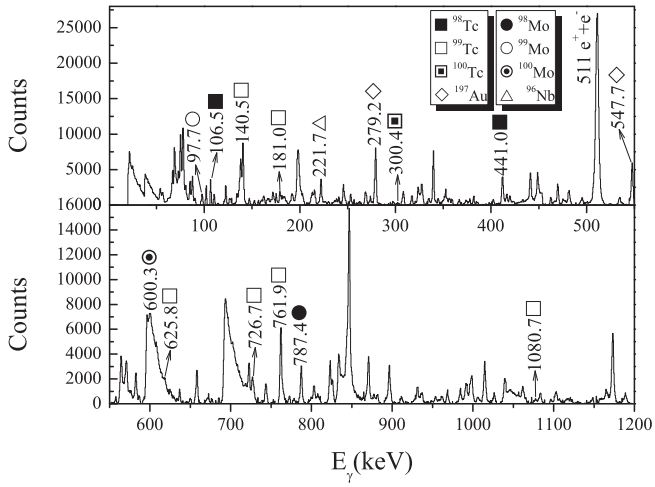

FIG. 1. Typical online γ-ray spectrum depicting the γ lines of different evaporation residues via complete fusion in the ^{6}Li + ^{96}Zr system at the bombarding energy of 28 MeV.

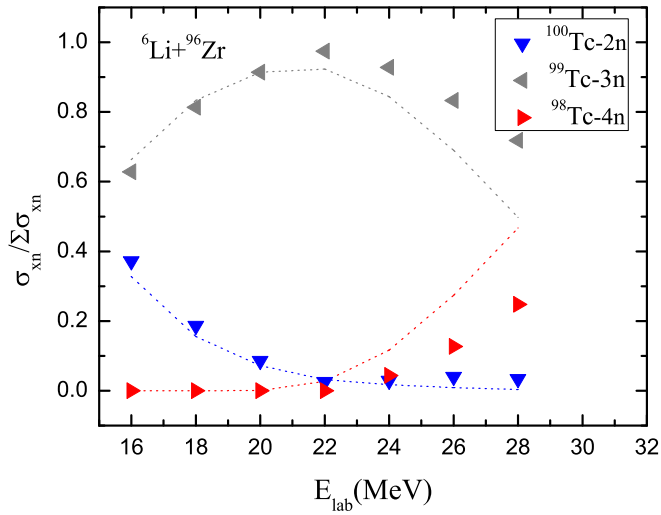

FIG. 2. (Color online) Ratio of individual channel cross sections to the CF cross sections as a function of beam energy for ^{6}Li + ^{96}Zr. The dot lines represent the theoretical estimation of PACE2.

III. DERIVATION of FUSION CROSS SECTIONS

The compound nucleus formed following the collision of ^{6}Li and ^{96}Zr is ^{102}Tc, which then decays predominantly by neutron evaporation, leading to different Tc isotopes. The dominant decay channels are observed to be $2n$, $3n$, and $4n$ evaporations at all energies, which agree well with a statistical model calculation using the code PACE2 [34]. The transitions feeding the ground state of the residues of CF, given in Table I, were identified and used in the calculations. For the $2n$ channel (^{100}Tc), the 300.4-keV transition is not to the ground state, but it is by far the highest intensity transition.

The fusion cross section for the online measurement is calculated using the relation

$$\sigma_\gamma = \frac{N_\gamma}{\varepsilon_\gamma N_B N_T}, \quad (1)$$

where ε_γ is the absolute efficiency of all the detectors for the γ lines, N_B and N_T represent the total number of beam particles incident on the target and the target atoms per unit area, respectively, and N_γ denotes the yield of the γ-ray peak after correcting with the internal conversion. The cross sections of individual residues equal to the sum of cross sections of all observed ground-state feeding transitions. It is to be mentioned that the intensities of some transitions were too small to be observed; thus the fraction of these γ rays is neglected for the present system. In order to obtain the relative contribution of other residue channels to CF, the statistical model code PACE2 was used for the calculations. The L distribution obtained from the CCFULL [38] calculations was used as an input of PACE2 at each energy.

$R_\delta^{\text{theory}} = \Sigma_x \delta_{\text{xn}}^{\text{PACE2}}/\delta_{\text{fus}}^{\text{PACE2}}$ (x = 2,3,4) was calculated and the results indicate that the summed cross sections of $2n$, $3n$, and $4n$ channels contribute from 96.8% to 99.4% of the complete fusion cross section for the ^{6}Li + ^{96}Zr system. Figure 2 shows the individual xn channel cross sections normalized to the CF cross sections for the reaction ^{6}Li + ^{96}Zr. A reasonable agreement between the $\sigma_{\text{xn}}^{\text{Pace}}$ and measured $\sigma_{\text{xn}}^{\text{Expt.}}$ is observed over the whole energy range. A better agreement with the relative percentage of the $3n$ and $4n$ channels might be obtained if we varied the level density parameter in the calculations. However, this procedure was not in the scope of the present work. As can be observed in Table II, the contributions of other evaporation residues to the total complete fusion are small and the total complete fusion

TABLE I. Characteristic γ rays of ^{98}Tc [35], ^{99}Tc [36], and ^{100}Tc [37] used in the calculation.

Residual channels	Transition	E_γ (keV)	I_γ (%)
^{98}Tc ($4n$)	$7^+ \longrightarrow 6^+$	441.0	100
	$7^+ \longrightarrow 6^+$	106.5	68.4
^{99}Tc ($3n$)	$13/2^+ \longrightarrow 9/2^+$	761.9	100
	$11/2^+ \longrightarrow 9/2^+$	726.7	31.4
	$9/2^+ \longrightarrow 9/2^+$	625.8	12.8
	$11/2^+ \longrightarrow 9/2^+$	1080.7	7.5
	$5/2^+ \longrightarrow 9/2^+$	181.0	14.8
	$7/2^+ \longrightarrow 9/2^+$	140.5	106.5
^{100}Tc ($2n$)	$6^- \longrightarrow 6^+$	300.4	100

TABLE II. The cross sections for $2n$-ER, $3n$-ER, $4n$-ER, and total complete fusion with R_δ^{theory} obtained from PACE2 calculations.

E_{lab} (MeV)	$E_{\text{c.m.}}$ (MeV)	$\sigma_{2n+3n+4n}^{\text{Expt.}}$	R_δ^{theory} (%)	$\delta_{\text{fus}}^{\text{exp}}$ (mb)
28.0	26.4	762.68 ± 48.28	96.8	787.57 ± 49.86
26.0	24.5	752.22 ± 47.70	97.3	773.10 ± 49.03
24.0	22.6	560.05 ± 35.96	97.8	572.59 ± 36.76
22.0	20.7	324.58 ± 20.78	98.2	330.43 ± 21.16
20.0	18.8	236.27 ± 15.82	98.6	239.53 ± 16.04
18.0	16.9	73.30 ± 5.35	98.9	74.12 ± 5.41
16.0	15.1	10.64 ± 1.52	99.1	10.74 ± 1.53

TABLE III. Characteristic γ rays used in the ICF calculation.

Residual channels	Transition	E_γ (keV)	I_γ (%)
^{98}Mo	$2^+ \longrightarrow 0^+$	787.4	100
^{99}Mo	$5/2^+ \longrightarrow 1/2^+$	97.7	75.1 (40)
^{100}Mo	$4^+ \longrightarrow 2^+$	600.3	100
^{96}Nb	$7^+ \longrightarrow 6^+$	221.7	100

cross section was derived by $\delta_{\rm fus}^{\rm exp} = \Sigma\delta_{\rm xn}^{\rm exp}/R_\delta^{\rm theory}$. A similar procedure was used to derive the ICF cross sections. However, for ICF we could only determine the lower limit for the cross sections, because some γ-ray lines corresponding to some evaporation channels were too weak above the background to be used for the cross section determination. Table III shows the characteristic γ lines used to derive the ICF cross sections. The ^{98,99,100}Mo nuclei are produced by neutron evaporation from the compound nucleus formed by absorption of an α particle by the target. The ^{96}Nb nucleus is produced by neutron evaporation from the compound nucleus formed by absorption of a proton or deuteron by the target. Table IV shows the cross sections for each of those evaporation channels. Table V shows the total CF and the lower limits of ICF and TF for the ^{6}Li + ^{96}Zr system. Figure 3 shows the experimental excitation functions obtained of CF and the lower limits of ICF and TF in the present work, for the ^{6}Li + ^{96}Zr system. ICF and TF correspond actually to a lower limit of the cross sections, as explained before. The not very smooth behavior of the ICF excitation function is due to the relative larger fraction of the cross section corresponding to the nonmeasured γ lines, which were more important at midenergies.

IV. DISCUSSION OF THE EFFECT OF BREAKUP AND TRANSFER CHANNELS ON THE FUSION CROSS SECTION

To investigate the effect of the breakup and transfer channels on the CF cross section data, we performed coupled channel calculations (CC) without taking into account breakup and transfer channels. By doing so, we consider that the differences between theoretical predictions and experimental results are due to coupling effects of the channels not included in calculations. As coupling effects related with the structure of the colliding nuclei and transfer channels are important

TABLE IV. The lower limits of cross sections for each of ICF evaporation channels of ^{6}Li+ ^{96}Zr system.

$E_{\rm lab}$ (MeV)	σ_f (^{98}Mo) (mb)	σ_f (^{99}Mo) (mb)	σ_f (^{100}Mo) (mb)	σ_f (^{96}Nb) (mb)
28.0	68.61 ± 4.24	61.78 ± 5.05	16.85 ± 1.96	24.62 ± 1.78
26.0	52.20 ± 3.36	58.58 ± 4.92	23.61 ± 2.19	22.13 ± 1.67
24.0	27.89 ± 1.97	30.41 ± 3.31	10.05 ± 1.47	11.04 ± 1.07
22.0	9.14 ± 0.75	14.73 ± 1.65	8.06 ± 0.85	5.45 ± 0.54
20.0	8.44 ± 0.93	25.33 ± 2.52	9.98 ± 1.17	5.59 ± 0.72
18.0	4.55 ± 0.55	11.20 ± 1.55	3.86 ± 0.70	1.85 ± 0.41
16.0	1.55 ± 0.30	2.91 ± 0.83	2.85 ± 0.47	1.02 ± 0.27

TABLE V. The cross sections of CF, lower limits of cross sections of ICF and TF for ^{6}Li+ ^{96}Zr system.

$E_{\rm lab}$ (MeV)	$\sigma_{\rm CF}$ (mb)	$\sigma_{\rm ICF}$ (mb)	$\sigma_{\rm TF}$ (mb)
28.0	787.57 ± 49.86	171.86 ± 10.83	959.43 ± 51.02
26.0	773.10 ± 49.03	156.52 ± 10.02	929.62 ± 50.04
24.0	572.59 ± 36.76	79.38 ± 5.71	651.97 ± 37.21
22.0	330.43 ± 21.16	37.38 ± 2.76	367.81 ± 21.34
20.0	239.53 ± 16.04	49.33 ± 3.79	288.86 ± 16.48
18.0	74.12 ± 5.41	21.46 ± 2.09	95.59 ± 5.79
16.0	10.74 ± 1.53	8.32 ± 1.12	19.07 ± 1.90

mostly at sub-barrier energies, the difference between data and coupled channels calculations will be attributed to the breakup process. In this kind of calculations, it is very important to adopt a reliable bare potential. For this reason we chose the widely used double-folding Sao Paulo potential (SPP) [39,40], which uses realistic densities and has no free parameters. In the coupled channel calculations, we included only the inelastic excitations of the targets. All coupled channel calculations were performed with the FRESCO code [41]. The ^{96}Zr excited states included in the CC calculations were the 2^+ and 3^- states at 1.76 and 1.90 MeV, respectively. The quadrupole deformation parameter used was $\beta_2 = 0.080$, taken from Ref. [42], and the octopole deformation parameter used was $\beta_3 = 0.235$, taken from Ref. [43]. The same values were assumed for nuclear and Coulomb deformations. For the real part of the optical potential the Sao Paulo potential was used [39,40]. For the imaginary part of the optical potential, we used a Woods-Saxon potential internal to the Coulomb barrier to account for the absorption of the flux that passes through or over the barrier (equivalent to the so-called ingoing wave boundary condition). The potential parameters were $W_0 = 50$ MeV, $r_0 = 1.06$ fm, and $a = 0.2$ fm for the depth, reduced radius, and diffuseness, respectively. We checked that the fusion cross section does not depend on the choice of these parameters,

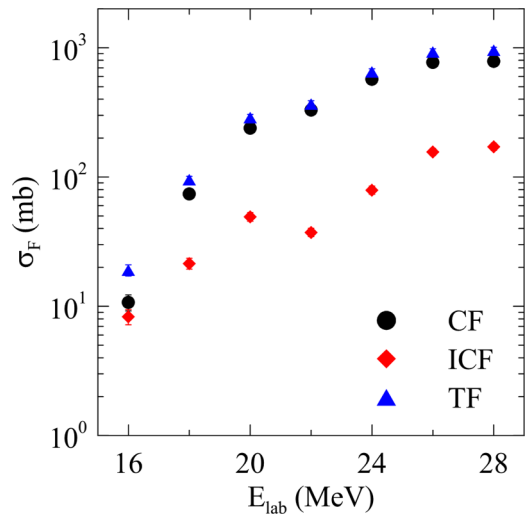

FIG. 3. (Color online) Measured complete, incomplete, and total fusion cross section at near the Coulomb barrier energies.

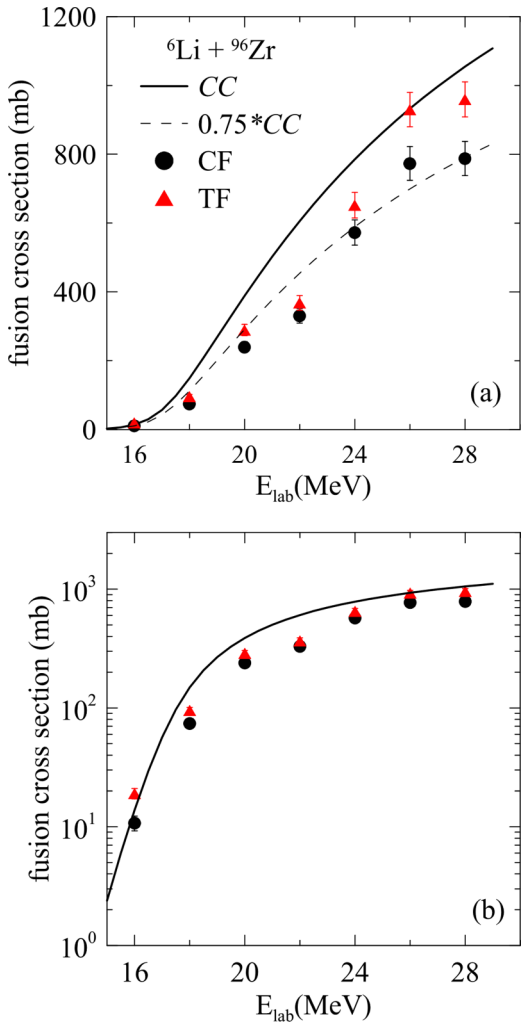

FIG. 4. (Color online) Complete and total fusion cross sections at energies near the Coulomb barrier for the ^{6}Li + ^{96}Zr system. The dashed line represents the coupled channel calculations multiplied by 0.75.

as long as the imaginary potential remains internal to the Coulomb barrier. In Figs. 4(a) and 4(b) we show the results of the calculations and the data for CF and TF in linear and logarithmic scales. The first is more suitable to observe the deviations at above-barrier energies, whereas the latter makes a zoom to observe the effects at low energies. One can observe in Fig. 4(a) that there is CF suppression of the order of 25%, at energies above the barrier, when compared with the coupled channel calculations. The lower limit of the TF cross section data is roughly in agreement with the calculations at the highest energies, which indicates that the ICF seems to be the responsible for the loss of flux going to CF, and consequently suppressing the CF at this energy regime. It is important to remember that the TF cross section may be larger than the derived one at some energies, as already explained in Sec. III.

One can observe that the CF suppression at energies slightly above the Coulomb barrier derived in the present work is smaller than the ones reported so far for the ^{6}Li projectile on heavier targets and also for the ^{90}Zr target. A possible reason for the difference concerning heavier targets has already been explored in the introduction of this paper: The small breakup probability for lighter targets may produce a smaller effect on the fusion cross section than for heavier targets. In the ^{90}Zr measured by Kumawat *et al.* [9] by off-line γ spectrometry method, they had larger uncertainties than us, since they could not measure all CF evaporation channels and therefore they had to rely strongly on predictions of the PACE code, which accounted for up to 40% of the derived CF cross sections. Our results are in reasonable agreement with the ones by Shaik *et al.* [28] for the ^{6}Li+ ^{64}Ni system, although those results also depend relatively strongly on PACE predictions. It should be very important to compare the CF suppression obtained in the present work with those of the available CF data of the ^{6}Li projectile with other targets, especially ^{90}Zr, using the same interaction potential, in order to investigate whether the observed difference in the CF suppression is due to the different potentials used. Actually, those calculations were already performed and are published in Ref. [14], where Wang *et al.* report systematic CF behavior for different systems using the Sao Paulo potential. The suppression found ^{6}Li-induced CF with heavy targets, including ^{90}Zr, is 40%, with all systems fitting very well the 40% suppression curve.

V. SUMMARY

We report the measurement of complete fusion cross sections for ^{6}Li+ ^{96}Zr system at energies in the range from slightly below to slightly above the Coulomb barrier. The method used was the online γ-ray method, which allowed the measurement of almost 100% of the CF. Furthermore, we measured the incomplete fusion cross sections, although not very precisely, because some of the γ-ray lines could not be measured. The complete fusion cross section at above-barrier energies was found to be suppressed by ~25% when compared with coupled channel calculations that do not take into account the breakup and transfer couplings. This is a value smaller than the present systematic results available for heavier targets. We do not think that this an unexpected result, but rather a signature that the dynamic breakup effect on the complete fusion depends on the target charge and that the present accepted independence of the target charge is due to the lack of complete fusion data for light systems, for which the suppression should be smaller.

ACKNOWLEDGMENTS

This work is supported by National Natural Science Foundation of China under Grants No. 11475013, No. 11035007, No. 11175011, No. 11375266, No. 11375267, No. 11305269, No. 11175259, No. 11475072, No.11405274, and No. 10775098, State Key Laboratory of Software Development Environment (SKLSDE-2014ZX-08), as well as the Fundamental Research Funds for the Central Universities and the Key Laboratory of High Precision Nuclear Spectroscopy, Institute of Modern Physics, Chinese Academy of Sciences. This work also benefited from discussions held at the CUSTIPEN. P.R.S.G. and J. Lubian thank the CNPq, CAPES, and FAPERJ for their financial support. The authors thank the

crew of the HI-13 tandem accelerator at the China Institute of Atomic Energy for steady operation of the accelerator. We are also grateful to Q. W. Fan for preparing the target. S. P. Hu and G. L. Zhang contributed equally to this work.

[1] L. F. Canto, P. R. Gomes, R. Donangelo, and M. S. Hussein, Phys. Rep. **424**, 1 (2006).
[2] N. Keeley, R. Raabe, N. Alamanos, and J. L. Sida, Prog. Part. Nucl. Phys. **59**, 579 (2007).
[3] J. Lubian *et al.*, Nucl. Phys. A **791**, 24 (2007).
[4] J. Lubian *et al.*, Phys. Rev. C **79**, 064605 (2009).
[5] S. Santra, S. Kailas, K. Ramachandran, V. V. Parkar, V. Jha, B. J. Roy, and P. Shukla, Phys. Rev. C **83**, 034616 (2011).
[6] M. Dasgupta *et al.*, Phys. Rev. C **70**, 024606 (2004).
[7] L. F. Canto *et al.*, Nucl. Phys. A **821**, 51 (2009).
[8] P. R. S. Gomes, J. Lubian, and L. F. Canto, Phys. Rev. C **79**, 027606 (2009).
[9] H. Kumawat *et al.*, Phys. Rev. C **86**, 024607 (2012).
[10] M. K. Pradhan *et al.*, Phys. Rev. C **83**, 064606 (2011).
[11] V. V. Parkar *et al.*, Phys. Rev. C **82**, 054601 (2010).
[12] V. Jha, V. V. Parkar, and S. Kailas, Phys. Rev. C **89**, 034605 (2014).
[13] L. R. Gasques, D. J. Hinde, M. Dasgupta, A. Mukherjee, and R. G. Thomas, Phys. Rev. C **79**, 034605 (2009).
[14] B. Wang, W.-J. Zhao, P. R. S. Gomes, E.-G. Zhao, and S.-G. Zhou, Phys. Rev. C **90**, 034612 (2014).
[15] D. R. Otomar, P. R. S. Gomes, J. Lubian, L. F. Canto, and M. S. Hussein, Phys. Rev. C **87**, 014615 (2013).
[16] M. S. Hussein, P. R. S. Gomes, J. Lubian, D. R. Otomar, and L. F. Canto, Phys. Rev. C **88**, 047601 (2013).
[17] N. T. Zhang *et al.*, Phys. Rev. C **90**, 024621 (2014).
[18] Y. D. Fang *et al.*, Phys. Rev. C **91**, 014608 (2015).
[19] D. H. Luong *et al.*, Phys. Lett. B **695**, 105 (2011).
[20] D. H. Luong *et al.*, Phys. Rev. C **88**, 034609 (2013).
[21] S. Santra *et al.*, Phys. Lett. B **677**, 139 (2009).
[22] A. Shrivastava *et al.*, Phys. Lett. B **633**, 463 (2006).
[23] C. S. Palshetkar, S. Santra, A. Chatterjee *et al.*, Phys. Rev. C **82**, 044608 (2010).
[24] J. Takahashi *et al.*, Phys. Rev. Lett. **78**, 30 (1997).
[25] A. Mukherjee *et al.*, Nucl. Phys. A **596**, 299 (1996); **635**, 305 (1998).
[26] A. Mukherjee *et al.*, Phys. Lett. B **526**, 295 (2002).
[27] A. Pakou *et al.*, J. Phys. G: Nucl. Part. Phys. **31**, S1723 (2005).
[28] Md. Moin Shaikh *et al.*, Phys. Rev. C **90**, 024615 (2014).
[29] I. Padron *et al.*, Phys. Rev. C **66**, 044608 (2002).
[30] P. R. S. Gomes *et al.*, Phys. Lett. B **601**, 20 (2004).
[31] A. di Pietro *et al.*, Phys. Rev. C **87**, 064614 (2013).
[32] C. Beck *et al.*, Phys. Rev. C **67**, 054602 (2003).
[33] L. F. Canto *et al.*, J. Phys. G **36**, 015109 (2009).
[34] A. Gavron, Phys. Rev. C **21**, 230 (1980).
[35] H. B. Ding *et al.*, Chin. Phys. Lett. **27**, 072501 (2010).
[36] G. Kajrys, W. DelBianco, S. Pilotte, S. Landsberger, and S. Monaro, Phys. Rev. C **31**, 409 (1985).
[37] P. Joshi *et al.*, Eur. Phys. J. A **24**, 23 (2005).
[38] K. Hagino, N. Rowley, and A. T. Kruppa, Comp. Phys. Commun. **123**, 143 (1999).
[39] L. C. Chamon, D. Pereira, M. S. Hussein, M. A. Candido Ribeiro, and D. Galetti, Phys. Rev. Lett. **79**, 5218 (1997).
[40] L. C. Chamon *et al.*, Phys. Rev. C **66**, 014610 (2002).
[41] I. J. Thompson, Comp. Phys. Rep. **7**, 167 (1988).
[42] S. Raman, C. W. Nestor Jr., and P. Tikkanem, At. Data Nucl. Data Tables **78**, 1 (2001).
[43] T. Kibedi and R. H. Spear, At. Data Nucl. Data Tables **80**, 35 (2002).